Effect of Lignin Particles as a Nucleating Agent on Crystallization of Poly(3-hydroxybutyrate)

Kai Weihua, Yong He, Naoki Asakawa, Yoshio Inoue

Department of Biomolecular Engineering, Tokyo Institute of Technology, Nagatsuta 4259, Midori-ku, Yokohama 226-8501, Japan

Received 17 November 2003; accepted 8 June 2004
DOI 10.1002/app.21204
Published online in Wiley InterScience (www.interscience.wiley.com).

ABSTRACT: The effect of lignin fine powder, as a new kind of nucleating agent, on the crystallization process of poly(3-hydroxybutyrate) (PHB) was studied. The kinetics of both isothermal and nonisothermal crystallization processes from the melt for both pure PHB and PHB/lignin blend was studied by means of differential scanning calorimetry. Lignin shortened the crystallization half-time $t_{1/2}$ for isothermal crystallization. The activation energy ΔE for PHB/lignin and pure PHB in the isothermal crystallization process was -237.40 and -131.22 kJ/mol, respectively, clearly indicating that the crystallization of the PHB/lignin blend was more favorable than that of pure PHB from a thermodynamic perspective. At the same time, according to polarized optical microscopy, the rate of spherulitic growth from the melt increased with the addition of lignin, which is ascribed to the reduction of surface fold energy σ_e, that is, σ_e is 59.2×10^{-3} and 41.6×10^{-3} J m^{-2} for pure PHB and PHB/lignin, respectively. Polarized optical microscopy also showed that the spherulites found in PHB with lignin were smaller in size and greater in number than those found in pure PHB. The wide-angle X-ray diffraction indicated that an addition of lignin caused no change in the crystal structure and degree of crystallinity. These results indicated that lignin is a good nucleating agent for the crystallization of PHB. © 2004 Wiley Periodicals, Inc. J Appl Polym Sci 94: 2466–2474, 2004

Key words: poly(3-hydroxybutyrate); lignin; nucleation; crystallization; biodegradable

INTRODUCTION

Poly(3-hydroxybutyrate) (PHB) is a naturally occurring polymer synthesized by various kinds of bacteria.[1,2] Because of its biodegradability, it has attracted much attention from not only biologists and chemists but also environmentalists and medical researchers.[1] However, the inherent brittleness impedes use of bacterial PHB as an engineering plastic.[3]

There are several possible causes of this brittleness. Because bacterially synthesized PHB is a completely isotactic stereoregular polyester, it has a high tendency to crystallize. However, the nucleation density of bacterial PHB is too low to initiate efficient crystallization. As a result, it forms spherulites of extremely large size.[4] After the first-stage crystallization from the melt of PHB, the secondary crystallization proceeds slowly at ambient temperature. This is partly attributed to its low glass-transition temperature (~ 5°C[5]). The large-size spherulite and secondary crystallization promote interspherulitic cracking during storage of the polymer at room temperature, which is commonly known to impair the mechanical properties of the materials.[4]

Correspondence to: Y. Inoue (yinoue@bio.titech.ac.jp).

Journal of Applied Polymer Science, Vol. 94, 2466–2474 (2004)

Many studies have been devoted to modifying the brittleness of PHB. Copolymerization[6–11] and blending[12–16] are used as common methods to overcome the brittleness of PHB. Copolymerizing 3-hydroxybutyrate with other hydroxyalkanoates, although it will improve the tensibility of PHB, will sometimes retard other preferable properties of PHB. For example, poly(3-hydroxybutyrate-*co*-3-hydroxyvalerate) has an improved tensibility, but the modulus of the material is sacrificed.[17] Because of poor miscibility of PHB with most polymers, blending PHB with other polymers scarcely leads to satisfactory results.[18–22]

Considering the drawbacks of methods mentioned above, modulation of crystallization behavior by a nucleating agent has become a promising method of improving the mechanical properties of PHB. By using a nucleating agent, it is expected that the nucleation density will increase and the size of spherulites will be reduced, thus greatly improving the tensibility of PHB, whereas the other desirable properties of PHB are not significantly impaired. In this regard, most materials used as nucleating agents are either inorganic or organic molecules, such as talc, boron nitride,[23] and saccharin.[13] Few works have reported macromolecules as nucleating agents, especially biodegradable macromolecules.

Lignin is one of the most abundant naturally occurring polymers and is obtained as a byproduct in the

pulp and paper industry.[24,25] Most of it is burned as an energy source, but there are some other potential uses for lignin, including applications as a filler or as a prepolymer in several polymeric systems.[26–28] The present article reports on the thorough investigation of the potential use of lignin as a nucleating agent of PHB. Lignin powder, with fine particle size, was selected because it meets several requirements as a nucleating agent in that it possesses many polar functional groups that can interact with PHB carbonyl and it has no melting point with a high glass-transition temperature.[27,29,30]

EXPERIMENTAL

Materials

The powder sample of biosynthesized isotactic PHB (MW ~ 200,000, Lot No. 06314C1, T_m = 172°C; Aldrich Chemical Co., Milwaukee, WI) was used as received. The lignin sample, in the form of a fine powder (Vanillex HW; Lot No. 98105152; MW ≅ 5000; average particle diameter 1.54 μm), was kindly supplied by the Nippon Paper Industries Co. Ltd. (Tokyo, Japan).

Preparation of PHB/lignin blend

The powders of dried lignin and PHB (1/99, w/w) were manually mixed thoroughly. The powder mixture was subsequently compression molded between poly(tetrafluoroethylene) sheets, with an appropriate spacer, for 3 min at 190°C under a pressure of 5 MPa, using a Mini Test Press-10 (Toyoseiki, Tokyo, Japan), followed by rapid cooling to room temperature between two iron plates. The blend samples (thickness: 0.2–0.3 mm) were aged at room temperature for 2 weeks before testing. For pure PHB films, PHB powder was directly compression molded into fine film.

Differential scanning calorimetry (DSC) analysis

The isothermal crystallization of PHB and PHB/lignin blend was studied by using a Pyris Diamond differential scanning calorimeter (DSC; Perkin Elmer Cetus Instruments, Norwalk, CT) in a nitrogen atmosphere. Calibration was carried out with an indium standard. For the isothermal crystallization, the as-mixed PHB/lignin samples were melted in the DSC cell at 190°C for 2 min, and then cooled rapidly to selected temperature for crystallization. During the isothermal crystallization process, the enthalpy change of the specimen was measured as a function of time.

The cold crystallization of the specimen, which was first melted at 190°C for 2 min and quickly quenched to below −50°C by liquid nitrogen, was conducted in the DSC cell at a heating rate of 10°C/min, on a Seiko DSC-20 differential scanning calorimeter (Seiko Instruments, Chiba, Japan) equipped with an SSC-580 thermal controller. The peak temperature, where the DSC cold crystallization curve reached its maximum, was taken as the cold crystallization temperature (T_{cc}).

The melt nonisothermal crystallization temperature (T_{mc}) was measured through crystallization from the melt on the Pyris Diamond DSC (Perkin–Elmer); the as-mixed sample was directly heated to 190°C in the DSC cell and held for 2 min, followed by cooling at a rate of 10°C/min until completion of hot crystallization. The peak temperature of the DSC melt crystallization curve was recorded as the T_{mc}.

Measurements of spherulitic growth rate by polarized optical microscopy (POM)

Spherulitic growth rates were measured by POM with an Olympus BX90 polarized microscope (Olympus, Osaka, Japan) equipped with a Mettler (Württ, Germany) FP82HT hot stage. The film samples were first heated from room temperature to 190°C and melted for 2 min. Subsequently, the samples were quenched to a selected crystallization temperature (T_c) and crystallized isothermally at T_c. Spherulitic radius of all the samples increased linearly with time. The value of spherulitic growth rate (G) was taken as the slope of the line obtained by plotting the spherulitic radius as a function of time.

Wide-angle X-ray diffraction (WAXD)

WAXD patterns were recorded in an incidence angle θ range of 5–55° at a scanning speed of 1°/min on an RU-200 X-ray diffractometer (Rigaku, Tokyo, Japan) at 40 kV/200 mA. The nickel-filtered Cu–K_α X-ray radiation (λ = 0.15418 nm) was used as the source. The degree of crystallinity was estimated according to the method of Vonk.[31]

RESULTS AND DISCUSSION

Isothermal crystallization

The isothermal crystallization of polymers can be described by an Avrami equation. The relative degree of crystallinity X_{rel} at time t is given by[32]

$$X_{rel} = \frac{X_c(t)}{X_c(\infty)} = \int_0^t \frac{dH(t)}{dt} dt \Big/ \int_0^\infty \frac{dH(t)}{dt} \qquad (1)$$

where $X_c(t)$ and $X_c(\infty)$ are the degree of crystallinity at time t and that at the end of crystallization, respectively; $dH(t)/dt$ is the rate of heat flow in the process of isothermal crystallization at time t. The time t was measured from the moment when the sample was

cooled to the appropriate crystallization temperature. X_{rel} can be obtained from the expression[32,33]

$$1 - X_{rel} = \exp(Kt^n) \quad (2)$$

Here n is the Avrami exponent, which is determined by the mode of crystal nucleation and the crystal growth geometry in the actual circumstance, and K is the parameter of isothermal crystallization rate. Taking a double logarithm of eq. (2) gives

$$\log[-\ln(1 - X_{rel})] = n \log t + \log K \quad (3)$$

The plot of $\log[-\ln(1 - X_{rel})]$ against $\log t$ gives a straight line, whose slope is n and intercept on the ordinate is $\log K$. In the experiments of isothermal crystallization at time t, $dH(t)/dt$, was recorded and then integrated against time t to give the values of $X_c(t)$ and $X_c(\infty)$.

When $X_{rel} = 0.5$ in eq. (3), the half crystallization time $t_{1/2}$, which is the time taken for 50% of total volume crystallization, is

$$t_{1/2} = \left(\frac{\ln 2}{K}\right)^{1/n} \quad (4)$$

Plots of $\log[-\ln(1 - X_{rel})]$ versus $\log t$ are shown in Figure 1. Each curve shows an initial linear portion in an early stage of crystallization and a later tendency to level off because of secondary crystallization.[34,35] The secondary stage is generally considered as the result of slower crystallization, crystal perfection, and/or spherulitic impingement in the later stage of crystallization process. In PHB samples, the secondary crystallization is mainly caused by the spherulitic impingement, which indicates that the form of crystal growth transformed from the primary crystallization into the secondary one. This secondary crystallization occurs in the interior of the dendrite or spherulite and fills in the void developed in the crystal. If the secondary crystallization is not completed, the product will continue to crystallize in the course of further uses, so to keep the shape and size of the PHB material stable during further use, it is very important to anneal the material under the temperature at which the crystallization rate becomes maximum for a sufficient length of time.

Also, for a given PHB sample, all the curves of the isothermal kinetics are almost parallel with each other. This indicates that the crystallization mechanism for the samples, at different crystallization temperatures, is the same. The values of n and K were determined from the initial linear portion in Figure 1 and are listed in Table I. The Avrami exponent n of PHB in the blend with lignin is between 2 and 3. According to the Avrami equation, in the ideal state of nucleated crystallization for three-dimensional crystallization

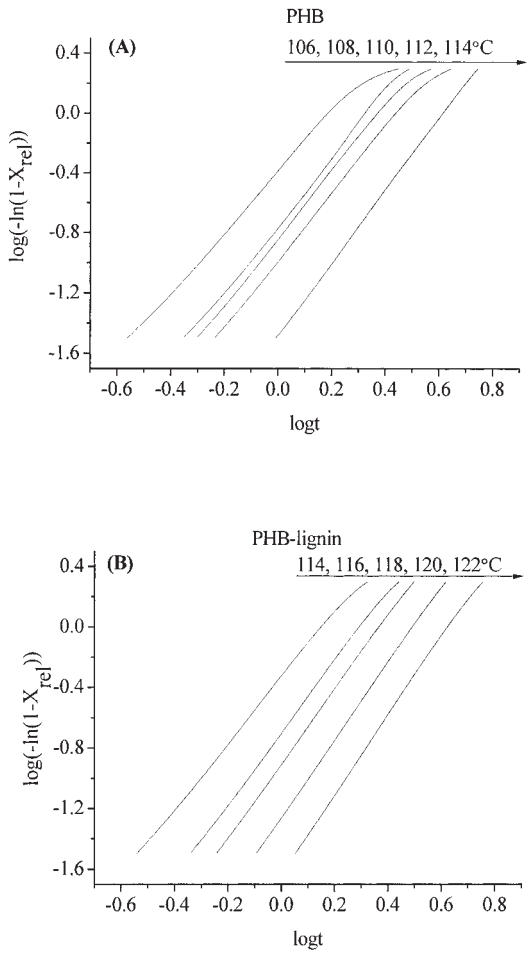

Figure 1 Isothermal kinetic curves for (A) pure PHB, (B) PHB/lignin (99/1) blend.

growth, the n value should be exactly 3.[32] In the actual process of crystal growth, however, the practical circumstance cannot satisfy the ideal state that the Avrami equation is supposed to have, causing the deviation of the n value from 3. For both pure PHB and PHB in the PHB/lignin blend, depression of the n value is probably attributable to the existence of athermal crystallization during the crystallization process. For the pure PHB sample, the value of K increases with decreasing crystallization temperature, whereas the $t_{1/2}$ value increases with increasing temperature. These results indicate that with increasing crystallization temperature, the crystallization rate decreases. It can be explained by the fact that melt crystallization exhibits the temperature dependency that is characteristic of nucleation-controlled crystallization associated with the proximity of T_m. A comparison of the K and $t_{1/2}$ values in pure PHB and in the PHB/lignin blend PHB, at the same crystallization temperature (114°C), shows that the K value of pure PHB is less than that of PHB in the blend with lignin, whereas the $t_{1/2}$ value shows the opposite trend, indicating that the crystallization rate of PHB in the blend with lignin is faster

TABLE I
Values of Avrami Parameters *n*, *K*, and $t_{1/2}$ for Isothermal Crystallization of PHB in the Pure State and in the PHB/Lignin (99/1) Blend

Sample	T_c (°C)	n	K ($\min^{-n}$)	$t_{1/2}$ (min)
Pure PHB	106	2.07 ± 0.02	0.414 ± 0.001	1.28 ± 0.01
	108	2.26 ± 0.03	0.176 ± 0.001	1.83 ± 0.02
	110	2.28 ± 0.02	0.146 ± 0.001	1.98 ± 0.01
	112	2.27 ± 0.01	0.103 ± 0.002	2.31 ± 0.01
	114	2.44 ± 0.01	0.032 ± 0.002	3.51 ± 0.01
PHB/lignin (99/1) blend	114	2.22 ± 0.02	0.471 ± 0.001	1.19 ± 0.01
	116	2.41 ± 0.02	0.200 ± 0.001	1.68 ± 0.01
	118	2.49 ± 0.01	0.124 ± 0.001	2.00 ± 0.01
	120	2.58 ± 0.01	0.054 ± 0.001	2.68 ± 0.01
	122	2.65 ± 0.01	0.023 ± 0.001	3.63 ± 0.01

than that of pure PHB at the same crystallization temperature.

Activation energy for isothermal crystallization (Δ*E*)

Given that the crystallization process for PHB is assumed to be thermally activated, the crystallization rate constant K can be approximately described by the following Arrhenius form[36]:

$$K^{1/n} = K_0 \exp(-\Delta E/RT_c) \tag{5}$$

$$\frac{1}{n}\ln K = \ln K_0 - \frac{\Delta E}{RT_c}$$

where K_0 is a temperature-independent preexponential factor, R is the gas constant, and ΔE is the activation energy of crystallization. ΔE can be determined as the slope coefficient by plotting $(1/n)\ln K$ against $1/T_c$ (Fig. 2). The value of ΔE for the primary crystallization process was found to be −131.22 kJ/mol for pure PHB and −237.40 kJ/mol for PHB in the blend with lignin. Because the energy should be released while transforming the molten fluid into the crystalline state, the sign of the ΔE value is negative. It is obvious that the crystallization of PHB in the lignin blend is promoted to a greater degree than that of pure PHB from a thermodynamic perspective because the former releases much more energy than the latter. This confirms that the introduction of lignin substantially increases the crystallization rate of PHB.

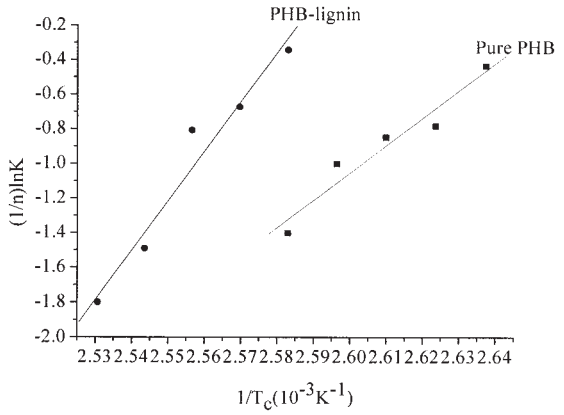

Figure 2 Plots of $(1/n)\ln K$ versus $1/T_c$ for Avrami parameter K deduced from isothermal crystallization for pure PHB and PHB–lignin blend.

Nonisothermal crystallization

The melt nonisothermal and cold crystallization temperature T_{mc} and T_{cc}, during dynamic cooling, are indirect measures of the crystallization rate. Usually, a lower T_{cc} indicates faster crystallization, whereas a lower T_{mc} indicates slower crystallization. T_{cc} and T_{mc} of pure PHB and PHB in the lignin blend were determined by DSC, and the results are shown in Figure 3. The T_{mc} and T_{cc} values of PHB samples shift to higher and lower temperatures, respectively, in the presence of lignin, whereas T_g values did not change. The increase in T_{mc} and the decrease in T_{cc} indicate that the addition of lignin significantly accelerates the crystallization of PHB, not only in the high-temperature region but also in the low-temperature region. At the same time, the crystallization peak of PHB in the blend with lignin became much sharper than those of pure PHB. Thus, it can be concluded that lignin could act as an effective nucleating agent for PHB.

The melt nonisothermal crystallization exotherms of PHB in the blend with lignin are presented in Figure 4. It can be seen that the peak temperature T_{mc} shifts to a lower-temperature region as the cooling rate Φ increases. The relative crystallinity X_t, as a function of crystallization temperature, is defined as

$$X_t = \frac{\int_{T_0}^{T}\left(\frac{dH_c}{dT}\right)dT}{\int_{T_0}^{T_\infty}\left(\frac{dH_c}{dT}\right)dT} \tag{6}$$

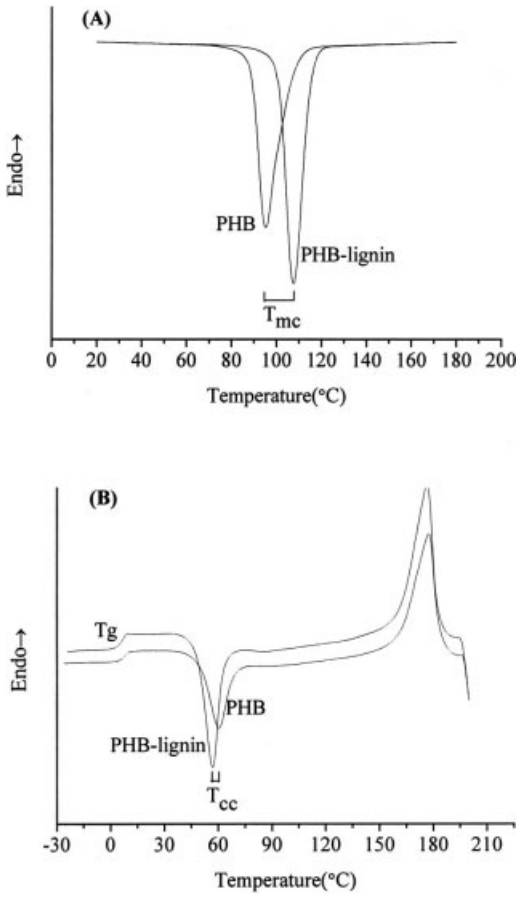

Figure 3 DSC cooling and heating curves of pure PHB and PHB–lignin blend samples: (A) cooling rate: −10°C/min (B) heating rate: 10°C/min.

where T_0 and T_∞ represent temperatures at the onset and the end of crystallization, respectively. During the melt nonisothermal crystallization process, the relation between crystallization time t and the corresponding temperature T is given by

$$t = \frac{T_0 - T}{\Phi} \tag{7}$$

According to eq. (6), the temperature-dependent relative crystallinity can be transformed into the time-dependent relative crystallinity.

Most methods for describing the melt nonisothermal crystallization kinetics are again based on a modified Avrami equation,[32,37] which assumes that the relative degree of crystallinity develops with crystallization time t, as follows:

$$1 - X_t = \exp(-Z_t t^n) \tag{8}$$

where the exponent n is a mechanism constant, depending on the type of nucleation and the growth process; and Z_t is a composite rate constant involving both nucleation and growth rate parameters. Considering the nonisothermal character of the process investigated, Jeziorny[38] pointed out that the value of Z_t should be adequately corrected. The factor to be considered is the cooling rate Φ. The final form of the parameter, characterizing the kinetics of melt nonisothermal crystallization, is given as follows:

$$\log Z_c = \frac{\log Z_t}{\Phi} \tag{9}$$

By using eq. (8), the values of $\log[-\ln(1 - X_t)]$ are plotted against $\log t$ for both PHB samples, as shown in Figure 5. Just the same as in isothermal crystallization, each curve shows an initial linear portion and subsequently tends to level off. The latter is attributed to the secondary crystallization caused by the spherulitic impingement in the later stages of crystallization process, as mentioned in the isothermal kinetic analysis. From the slope and the intercept of the linear part of the lines in Figure 5, the Avrami index n and rate constant Z_c, for both pure PHB and PHB in the blend with lignin, can be determined. The half-time $t_{1/2}$ for crystallization was obtained by an equation similar to eq. (4). All the data are listed in Table II. The values of n for melt nonisothermal crystallization are higher than those for isothermal crystallization (stated above) for both kinds of PHB samples. As known, the Avrami equation assumes that, during the crystallization process, the nucleation rate remains constant, although the nucleation rate during crystallization is actually temperature dependent. When the sample undergoes an isothermal crystallization, the nucleation rate remains constant, although when the sample undergoes a melt nonisothermal crystallization, it is no longer constant. So, higher values of n for the melt nonisothermal crystallization are attributed to much more complicated processes occurring during the melt nonisothermal crystallization. In addition, the values

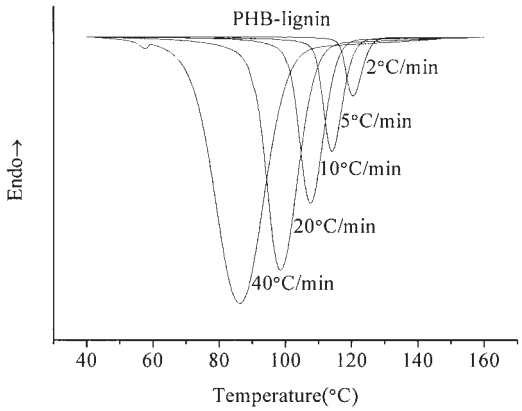

Figure 4 Nonisothermal crystallization DSC curves of PHB–lignin blend at various cooling rates of 2–40°C/min.

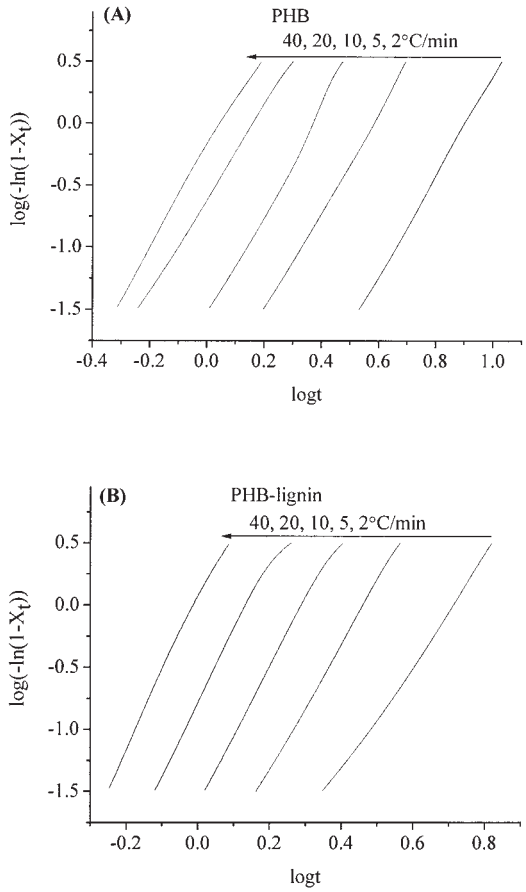

Figure 5 Nonisothermal kinetics curves for (A) pure PHB and (B) PHB–lignin blend obtained at various cooling rates of 2–40°C/min.

of half-time in the melt nonisothermal crystallization process did not show regular results as in the isothermal process. This is probably a result of different crystallization temperature ranges for pure PHB and the PHB/lignin blend in the melt nonisothermal crystallization process at a given cooling rate. The temperature range of the crystallization of the PHB/lignin blend is located at a much higher region than that of pure PHB, at a given cooling rate, as indicated in Figure 3(A).

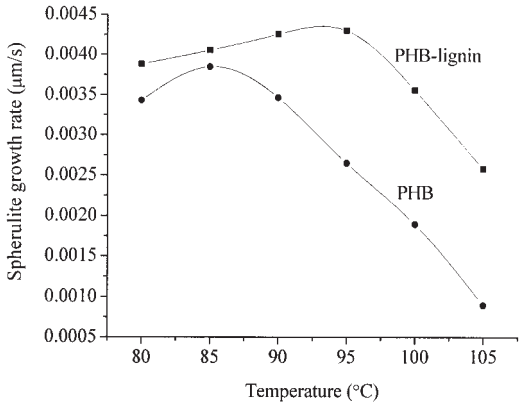

Figure 6 Spherulitic growth rate at various crystallization temperatures for both pure PHB and PHB–lignin blend.

Growth rate analysis and nucleation density of spherulites

The spherulitic growth rate (G) of PHB was measured as a function of isothermal crystallization temperature. The diameter of the PHB spherulite increases linearly with increasing time. As shown in Figure 6, with increasing temperature, the isothermal growth rate of both kinds of PHB samples first increases, reaches a maximum, and then decreases. This can be explained by the model of spherulitic growth proposed by Keith and Padden.[39] The G value first increases with the temperature because, in this temperature range, spherulitic growth is under the control of segmental diffusion. The following decrease of G value is attributed to a change of the dominant factor controlling spherulitic growth from a segmental diffusional control to a nucleus formation control in the higher-temperature region. Figure 6 also shows that

TABLE II
Values of Avrami Parameters n, Z_c, and $t_{1/2}$ for Melt Nonisothermal Crystallization of PHB in the Pure State and in the PHB/Lignin (99/1) Blend

Sample	Φ (°C/min)	n	Z_c (min^{-n})	$t_{1/2}$ (min)
Pure PHB	2	4.16 ± 0.01	0.013 ± 0.001	2.58 ± 0.02
	5	3.89 ± 0.01	0.349 ± 0.001	1.19 ± 0.01
	10	4.08 ± 0.01	0.697 ± 0.001	1.00 ± 0.01
	20	3.78 ± 0.01	0.932 ± 0.001	0.93 ± 0.01
	40	4.22 ± 0.01	0.991 ± 0.001	0.90 ± 0.01
PHB/lignin (99/1) blend	2	4.14 ± 0.01	0.032 ± 0.001	2.10 ± 0.02
	5	5.09 ± 0.01	0.339 ± 0.001	1.15 ± 0.01
	10	5.63 ± 0.01	0.690 ± 0.001	1.00 ± 0.01
	20	6.02 ± 0.01	0.914 ± 0.001	0.96 ± 0.01
	40	6.40 ± 0.02	1.007 ± 0.001	0.94 ± 0.01

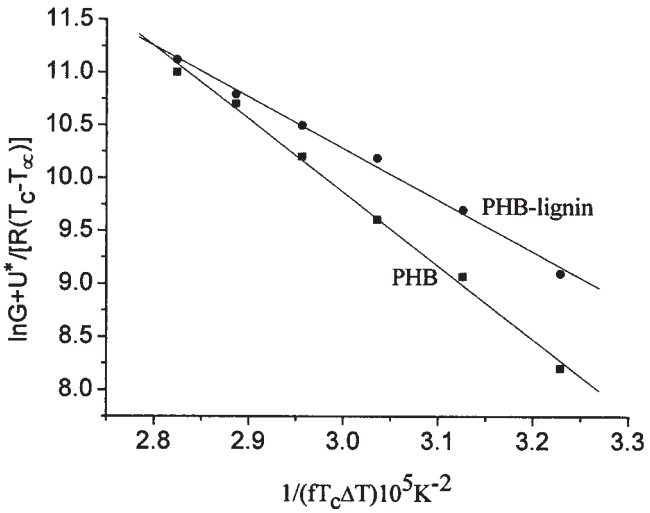

Figure 7 Lauritzen–Hoffman plot for PHB and PHB–lignin blend.

the maximum spherulitic growth rate of PHB in the blend with lignin is higher than that of pure PHB and it shifts to a higher crystallization temperature region. This observation can be explained by the occurrence of increased nucleation ability by the introduction of lignin.

According to Hoffman's nucleation theory of isothermal crystallization, the dependency of growth rate G on the crystallization temperature T_c and on the excessive cooling degree, $\Delta T = T_m^\circ - T_c$, is described by the following equation[40]:

$$G = G_0 \exp\left[-\frac{U^*}{R(T_c - T_\infty)}\right] \exp\left(-\frac{K_g}{fT_c\Delta T}\right) \quad (10)$$

where G_0 is a preexponential factor not strongly dependent on the temperature; R is the gas constant; T_∞ is a theoretical temperature at which all motion associated with viscous flow ceases ($T_\infty = T_g - C$; C = constant); T_m° is the equilibrium melting temperature, at which the polymer chains in the crystalline region gain motion and the crystals begin to soften; and f is the correction factor for temperature dependency of heat of fusion and is written as $f = 2T_c/(T_m^\circ + T_c)$.

U^* is the activation energy of the polymer segments transporting to the crystal front through the subcooled melt, which can be calculated with the Williams–Landel–Ferry relation[41]

$$U^* = \frac{C_1 T_c}{C_2 + T_c - T_g} \quad (11)$$

where C_1 and C_2 are constants (generally assumed to be 4120 cal/mol and 51.6 K, respectively).[42]

K_g is a nucleation constant for a given growth regime, which is given as[43]

$$K_g = \frac{nb_0\sigma\sigma_e T_m^\circ}{\Delta H^\circ k} \quad (12)$$

where b_0 is the thickness of a monomolecular layer, and σ and σ_e are the lateral and the fold surface free energies, respectively. ΔH° is the heat of fusion of completely crystalline PHB and k is the Boltzmann constant. According to the Hoffman–Lauritzen theory, the value of n depends on the regime of crystallization. The n value is 4, when T_c values lie in regime I (lower ΔT) or regime III (higher ΔT), and is 2 for the regime II growth process (medium ΔT).

A plot of $\ln G + U^*/[R(T_c - T_\infty)]$ versus $(1/T_c \times f \times \Delta T)$ with T_m° value (470 K) and $U^* = 10{,}250$ J/mol, obtained from the result reported by Barham et al.,[44] shows straight lines for neat PHB and PHB in the blend with lignin. The results are shown in Figure 7. The values of K_g, calculated from the slopes, are listed in Table III, from which it is seen that the value of K_g of neat PHB was greater than that of the PHB/lignin blend. The nucleation constant K_g represents the free energy necessary to form a nucleus of critical size, so it can be concluded that PHB in the blend with lignin needs less energy to form the nucleus of critical size.

Barham et al.[44] found that the n value of neat PHB was 4 and its isothermal crystallization behavior was assigned to regime III. The crystallization of PHB in the blend with lignin was considered to occur in regime III. This result is similar to results previously reported by Liu et al.[45] Using the empirical relation,[46]

$$\sigma = \alpha \Delta H_f (a_0 b_0)^{1/2} \quad (13)$$

and eq. (12), σ_e can be calculated. Here, α is an empirically determined constant. Taking $\alpha = 0.25$ for high-melting polyesters, and using the values of $a_0 = 6.6$ Å, $b_0 = 5.8$ Å, and $\Delta H_f = 1.85 \times 10^8$ J m^{-3},[47] the σ value is estimated to be 28.6×10^{-3} J m^{-2}. Thus, the σ_e value is calculated as 59.2×10^{-3} J m^{-2} for neat PHB, which agrees fairly well with the reported value 58.7×10^{-3} J m^{-2}.[48] Using the same values, $\alpha = 0.25$, $a_0 = 6.6$, $b_0 = 5.8$, and $\Delta H_f = 1.85 \times 10^8$ for PHB in the blend with lignin, the σ_e value was calculated to be 41.6×10^{-3} for PHB in the blend with lignin, indicating a decrease in the σ_e value by adding lignin. A decrease of surface free energy indicates that lignin provides a surface

TABLE III
Values of K_g and σ_e

Sample	K_g (10^5 K^2)	σ_e (10^{-3} J m^{-2})
Pure PHB	6.94 ± 0.22	59.2 ± 1.8
PHB–lignin	4.87 ± 0.18	41.6 ± 1.5

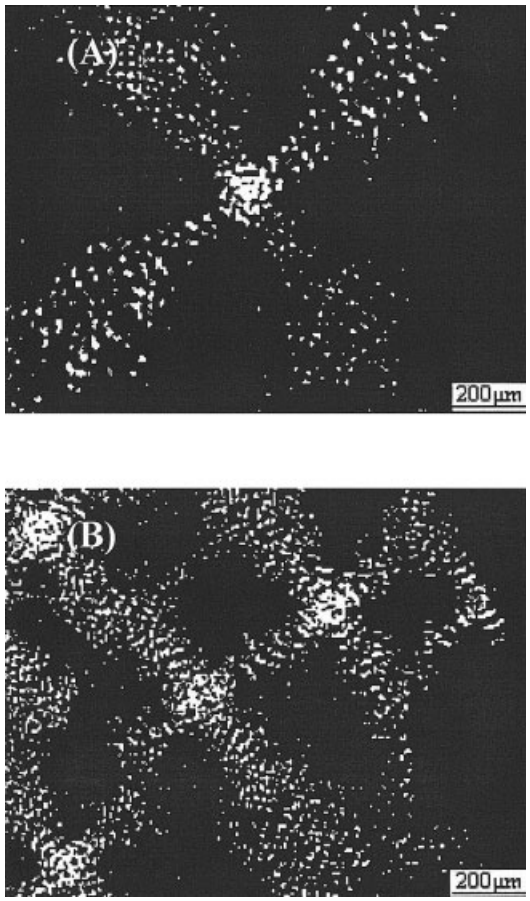

Figure 8 Polarized optical microphotographs of (A) pure PHB and (B) PHB–lignin blend isothermally crystallized at 110°C.

that reduces the free energy barrier to primary nucleation of PHB. Figure 8 shows the polarized optical microphotographs for PHB samples crystallized at T_c = 110°C. The spherulites of neat PHB are larger in size and smaller in numbers than those of PHB/lignin blend. These results prove that, as a nucleating agent, lignin not only reduces the energy barrier for PHB crystallization but also increases the nucleation density. This might be explained by a heterogeneous nucleation initiated with the introduction of lignin into PHB. The PHB segment has the ability to form hydrogen bonds with lignin polar groups.[27,30] These hydrogen-bonded PHB segments may act as the true nucleating agent to initiate nucleation. Heterogeneous nucleation decreases the surface energy barrier and increases the nucleation density for PHB crystallization. It is therefore natural that the crystallization rate of PHB increases with the introduction of lignin particle into PHB.

Crystalline structure and crystallinity

Figure 9 shows the WAXD patterns of both kinds of PHB samples. The WAXD pattern of neat PHB is similar to that of PHB in the blend with lignin, indicating that there is no crystalline structural change with the introduction of lignin into PHB. The degrees of crystallinity of PHB determined from the WAXD are 63 and 61% for neat PHB and PHB in the blend with lignin, respectively, indicating no noticeable change in crystallinity with the introduction of lignin and, thus, the introduction of lignin as a nucleating agent will not change the crystalline structure as well as the crystallinity of PHB.

CONCLUSION

In this work, the effect of lignin on the crystallization of PHB was studied. It was found that lignin particles constitute a good nucleating agent for PHB.

DSC data showed that, with the introduction of lignin, the crystallization peak temperature increased in the nonisothermal melt-crystallization process and decreased in the cold-crystallization process, and that the half-crystallization time for the isothermal crystallization is shortened. According to the POM observation, the spherulitic growth rate, the maximum spherulitic growth temperature, and the nucleation density increased with the introduction of lignin. Further X-ray studies showed that the crystalline structure and crystallinity did not change with the addition of lignin.

For the nonisothermal crystallization, lignin particles decreased the nucleus formation barrier energy in the high crystallization region and increased the PHB segmental mobility in the low-temperature region. The deduced surface fold energy σ_e, 59.2×10^{-3} and 41.6×10^{-3} J m^{-2} for neat PHB and PHB in the blend with lignin, respectively, and increased nucleation density supported the conclusion that lignin acted as a good nucleating agent for PHB. PHB segments can form hydrogen bonds with lignin polar groups and these hydrogen-bonded PHB segments may initiate heterogeneous nucleation in the crystallization pro-

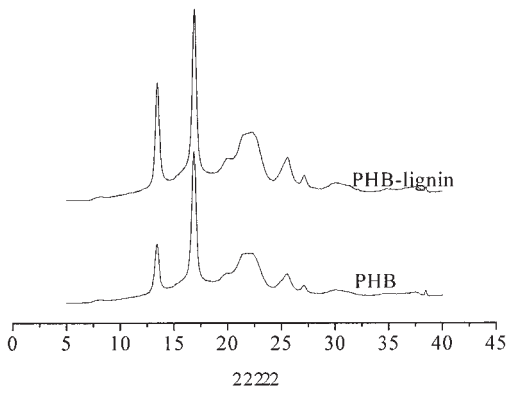

Figure 9 Wide-angle X-ray diffraction patterns for pure PHB and PHB–lignin blend.

cess of PHB. Lignin is one of the most abundant naturally occurring polymers, and is obtained as a by-product in the pulp and paper industry, which makes it very cheap to use. Moreover, it is biodegradable and safe to the environment, thus making lignin a promising nucleating agent.

References

1. Holmes, P. A. Phys Technol 1985, 16, 32.
2. Doi, Y.; Tamaki, A.; Kunioka, M.; Soga, K. Appl Microbiol Biotechnol 1988, 28, 330.
3. De Koning, G. J. M.; Lemstra, P. J. Polymer 1993, 34, 4089.
4. El-Hadi, A.; Schnabel, R.; Straube, E.; Müller, G.; Henning, S. Polym Test 2002, 21, 665.
5. Inoue, Y.; Yoshie, N. Prog Polym Sci 1992, 17, 571.
6. Madden, L. A.; Anderson, A. J.; Astar, J. Macromolecules 1998, 31, 5660.
7. Braunegg, G.; Lefebvre, G.; Genser, K. F. J Biotechnol 1998, 65, 127.
8. Shi, F.; Ashby, R. D.; Gross, R. A. Macromolecules 1997, 30, 2521.
9. Doi, Y.; Kitamura, S.; Abe, H. Macromolecules 1995, 28, 4822.
10. Abe, H.; Doi, Y.; Aoki, H.; Akehata, T.; Hori, Y.; Yamaguchi, A. Macromolecules 1995, 28, 7630.
11. Inoue, Y. J Mol Struct 1998, 441, 119.
12. Verhoogt, H.; Ramsay, B. A.; Favis, B. D. Polymer 1994, 35, 5155.
13. Avella, M.; Martuscelli, E.; Raimo, M. Polymer 1993, 34, 3234.
14. Greco, P.; Martuscelli, E. Polymer 1989, 30, 1475.
15. An, Y.; Li, L.; Dong, L.; Mo, Z.; Feng, Z. J Polym Sci Part B: Polym Phys 1999, 37, 443.
16. Inoue, Y. In: Solid State NMR of Polymers; Ando, I.; Asakura, T., Eds.; Biodegradable Polymers; Elsevier: Amsterdam, 1998; Chapter 21.
17. Barham, P. J.; Organ, S. J. J Mater Sci 1994, 29, 1676.
18. Gassner, F.; Owen, A. J. Polymer 1992, 33, 2508.
19. Iriondo, P.; Iruin, J. J.; Fernandez-Berridi, M. J. Polymer 1995, 36, 3235.
20. Yuan, Y.; Ruckenstein, E. Polymer 1998, 39, 1893.
21. Yoshie, N.; Azuma, Y.; Sakura, M.; Inoue, Y. J Appl Polym Sci 1995, 65, 17.
22. Azuma, Y.; Yoshie, N.; Sakura, M.; Inoue, Y.; Chujo, R. Polymer 1992, 33, 4763.
23. Withey, R. E.; Hay, J. N. Polymer 1999, 40, 5147.
24. Feldman, D.; Baru, D.; Luchian, C.; Wang, J. J Appl Polym Sci 1991, 42, 1537.
25. Simionescu, C. I.; Rusan, V.; Macoveanu, M. M.; Cazacu, G.; Lipsa, R.; Vasile, C.; Stoleriu, A.; Ioanid, A. Compos Sci Technol 1993, 48, 317.
26. Matte, J. F.; Doucet, J. Cellul Chem Technol 1988, 22, 71.
27. Li, J.; He, Y.; Inoue, Y. Polym Int 2003, 52, 949.
28. Baumberger, S.; Lapierre, C.; Monties, B.; Della Valle, G. Polym Degrad Stab 1998, 59, 273.
29. Myrvold, B. O.; Pavlov, D. J Power Sources 2000, 85, 92.
30. Li, J.; He, Y.; Inoue, Y. Polym J 2001, 33, 336.
31. Vonk, C. G. J Appl Crystallogr 1970, 42, 76.
32. Avrami, M. J Chem Phys 1940, 8, 212.
33. Binsbergen, F. L. J Macromol Sci B 1970, 4, 837.
34. Wunderlich, B. Macromolecular Physics, Vol. 2; Academic Press: New York, 1977.
35. Liu, J. P.; Mo, Z. S. Chin Polym Bull 1991, 4, 199.
36. Cebe, P.; Hong, S.-D. Polymer 1986, 27, 1183.
37. Avrami, M. J Chem Phys 1939, 7, 1103.
38. Jeziorny, A. Polymer 1978, 19, 1142.
39. Keith, H. D.; Padden, F. J. J Appl Polym Sci 1986, 32, 2919.
40. Hoffman, J. D. Polymer 1983, 24, 3.
41. Williams, M. L.; Landell, R. F.; Ferry, J. D. J Am Chem Soc 1995, 77, 3701.
42. Zhong, Z. K.; Guo, Q. P. J Polym Sci Part B: Polym Phys 1999, 37, 2726.
43. Hoffman, J. D.; Davis, G. T.; Lauritzen, J. I. In: Treatise on Solid State Chemistry, Vol. 3; Hennay, N. B., Ed.; Plenum: New York, 1975; Chapter 6.
44. Barham, P. J.; Keller, A.; Otun, E. L.; Holmes, P. J Mater Sci 1984, 19, 2781.
45. Liu, W. J.; Yang, H. L.; Wang, Z.; Dong, L. S.; Liu, J. J. J Appl Polym Sci 2002, 86, 2145.
46. Lauritzen, J. I.; Hoffman, J. D. J Appl Phys 1973, 44, 4340.
47. Pearce, R.; Brown, G. R.; Marchessault, R. H. Polymer 1994, 35, 3984.
48. Zhang, L. L.; Goh, S. H.; Lee, S. Y.; Hee, G. R. Polymer 2000, 41, 1429.